ELSEVIER

Physica D 170 (2002) 131–142

PHYSICA D

www.elsevier.com/locate/physd

DC currents in Hamiltonian systems by Lévy flights

S. Denisov [a,*], J. Klafter [a], M. Urbakh [a], S. Flach [b]

[a] *School of Chemistry, Tel Aviv University, Tel Aviv 69978, Israel*
[b] *Max-Planck-Institut für Physik Komplexer Systeme, Nöthnitzer Str. 38, D-01187 Dresden, Germany*

Received 7 November 2001; received in revised form 7 May 2002; accepted 8 May 2002
Communicated by E. Ott

Abstract

We study the mechanism leading to directed transport in the stochastic layer of AC-driven Hamiltonian systems. We show that current rectification is obtained by breaking the symmetry of Lévy flights in ballistic channels which exist due to resonance islands with nonzero winding numbers. In the framework of the continuous time random walk (CTRW) approach, we construct a generalized asymmetric flights model and derive an expression for the current in terms of the characteristics of the relevant ballistic channels. We find very good agreement between the results of direct integration of the dynamical equations and the CTRW formulation.

PACS: 05.40.+j; 05.45.Ac; 05.60.Cd

Keywords: Hamiltonian systems; Lévy flights; Directed transport

1. Introduction

Transport properties of dynamical systems have been a subject of interest over a long period of time [1]. Recently, a new feature of such transport has been discussed: directed current (DC) which is produced by breaking time and/or spatial symmetries in dynamical systems, without applying an external constant bias and gradients [2–6]. Initially, inspired by studies of ratchets [7], the phenomenon of DC currents produced by dynamical asymmetries covers a broad class of physical systems, e.g. underdamped Josepshon junctions [8], cold atoms systems [9,10], etc. For these systems inertia effects are essential, in contrast to canonical overdamped models, in which inertia contributions are negligible due to high viscosity at the microscopic scale [7].

The presence of inertia may qualitatively change the picture: (a) low-dimensional chaos in underdamped nonlinear systems can play effectively the role of thermodynamic fluctuations, as in the case of deterministic diffusion [11]; (b) inertia terms induce dynamical correlations which may lead to new mechanisms of current rectification [12].

The mechanisms of current generation in dissipative nonlinear systems have been studied in detail [3,4,6]. It has been shown that these effects are determined by breaking the symmetry of limit cycle attractors basins [3], the

* Corresponding author.
E-mail address: denysov@post.tau.ac.il (S. Denisov).

0167-2789/02/$ – see front matter © 2002 Published by Elsevier Science B.V.
PII: S0167-2789(02)00545-6

existence of uncompensated ballistic limit cycles [6] and the asymmetry of chaotic attractors [4]. In contrast, the case of Hamiltonian dynamical systems is much less understood [13]. In Ref. [3], it has been shown that breaking of time and/or spatial symmetries leads to the appearance of a strong DC current in the chaotic layer of an AC-driven Hamiltonian system. Recently, an approach has been proposed that allows to estimate the mean value of a DC current [14]. Moreover, the analysis of the corresponding kinetic equations shows that upon approaching the dissipationless (Hamiltonian) limit, the value of the induced DC current is enhanced by several orders of magnitude [15].

In this work, we study the microscopic dynamical mechanism of current rectification in an AC-driven Hamiltonian system. Detailing the conclusions briefly exposed in Ref. [16], we demonstrate that directed current is induced by breaking of symmetry of Lévy flights which are induced by the presence of resonance islands embedded into the chaotic layer (these are basically Lévy walks due to presence of velocity [17,18]). Thus, like in the case of anomalous Hamiltonian diffusion [18,19], the direction and magnitude of the current are determined by the structure of ballistic resonances, namely by resonances with nonzero winding numbers υ. The quantitative measure of the asymmetry of the resonance structure is given by probability distribution functions (PDFs) of sticking times calculated for resonances embedded into the chaotic layer. The lack of symmetries means that these PDFs cannot be ordered in pairs $\{\psi_i(t) = \psi_j(t),\ \upsilon_i = -\upsilon_j\}$. Using the notion of ballistic flights and the continuous time random walk (CTRW) framework, we construct an asymmetric Lévy flights model, from which we derive an expression for the current as a sum over all relevant resonances.

The paper is organized as follows. In Section 2, we introduce the model and discuss relevant symmetries. Section 3 is devoted to the analysis of the relationship between current generation and flights, induced by ballistic resonances. Using the propagator for a given time, we detect the relevant resonances which form ballistic channels inside of chaotic layer. In Section 4, we introduce a generalized asymmetric CTRW approach and derive an expression for the current value as a sum over all ballistic channels (the details are given in Appendix A). We find a very good agreement between the results of CTRW formulation and the direct numerical integration of the dynamical equations. The main results are summarized in Section 5, together with a discussion of possible applications of this model to physical phenomena.

2. The model and relevant symmetries

A relatively simple Hamiltonian model, which can be used to demonstrate the presence of an asymptotically constant current without any constant bias and gradients, is the system of a particle moving in a spatially periodic potential $U(x)$, $U(x + L) = U(x)$ under the influence of time-periodic zero-mean force $E(t)$, $E(t + T) = E(t)$, $\langle E(t)\rangle = 0$:[1]

$$H = \frac{p^2}{2} + U(x) - xE(t), \qquad \ddot{x} = -\frac{\partial U(x)}{\partial x} + E(t), \tag{1}$$

where L and T are the spatial and temporal periods.

The Hamiltonian in Eq. (1), with a three-dimensional phase space, is generically non-integrable and is thus characterized by the presence of a stochastic layer which replaces the separatrix of the undriven integrable system. At the same time it contains regular trajectories, which are ballistic-like for large particle energies. The existence of these trajectories, which can be easily obtained when neglecting the potential $U(x)$ in Eq. (1), means that unbounded pumping of energy into the system through the field $E(t)$ is impossible. We will be interested in the dynamical properties of trajectories in the above-mentioned main stochastic layer, which corresponds to the dynamical states with the lowest energy.

[1] For another example of driving Hamiltonian see, e.g. [20].

As argued in Ref. [3], the ergodic properties of the stochastic layer allow to apply symmetry considerations which can be used to predict whether the trajectories have a zero average velocity. Note that symmetry breaking is a necessary but not a sufficient condition for the appearance of a DC current. The simple idea behind the symmetry analysis is to find all the symmetries of Eq. (1) which leave the equations of motion invariant but change the sign of the velocity $\dot{x}$. Since such symmetry operations map a given trajectory onto another one, by making sure that both trajectories belong to the same stochastic layer, and recalling the ergodic properties of the layer, we may immediately conclude that the average velocity in each trajectory from the chaotic area will be exactly zero. This symmetry approach has in fact been successfully applied to the general case of dissipative systems [3] which are also coupled to a heat bath [16].

For the system in Eq. (1), the possible symmetries are [3]

$$\hat{S}_1 : x \to -x,\ t \to t + \tfrac{1}{2}T, \qquad \{F(-x) = -F(x),\ E(t + \tfrac{1}{2}T) = -E(t)\}, \tag{2}$$

$$\hat{S}_2 : x \to x,\ t \to -t, \qquad \{E(-t) = E(t)\}, \tag{3}$$

where $F(x) = -\partial U(x)/\partial x$.

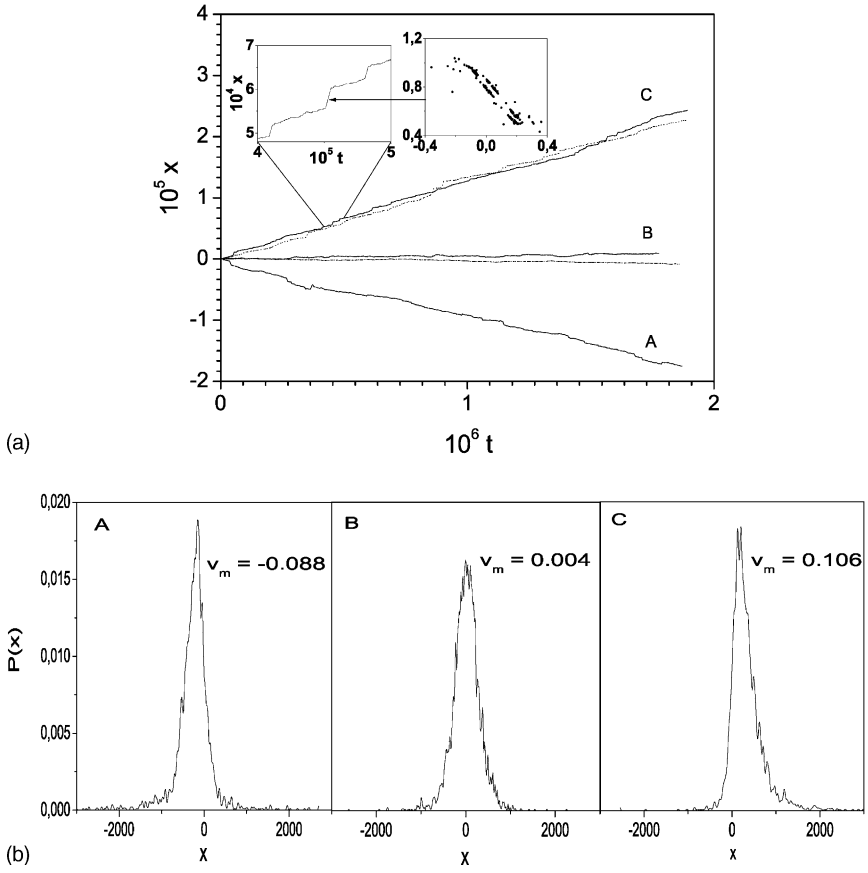

Fig. 1. (a) $x(t)$ versus t for different values of the third harmonic amplitude ($E_1 = 0.2$, $E_2 = -0.4$, $\phi_2 = 0.4$, $\phi_3 = 0$): $E_3 = 0$, $J \approx -0.1$ (case A); $E_3 = 0.143$, $J = 0$ (case B); $E_3 = 0.3$, $J \approx 0.12$ (case C). Left upper inset: zooming of $x(t)$ for the case C. Right inset shows the Poincaré section which corresponds to the longest flight in the blown up part of trajectory. The dashed curve corresponds to a filtered trajectory without flights (see text) and the dotted one corresponds to the CTRW simulation. (b) Spatial distribution of a particle ensemble $N = 10^4$ (see text) after time $t = 500T$. The mean velocities are determined as $v_m = (1/500T)\sum_{i=1}^{N} x_i(t = 500T)$.

The conditions in the brackets are the requirements for the periodic functions $U(x)$ and $E(t)$. The way to break the symmetries is to choose functions $U(x)$ and $E(t)$ which violate the listed requirements. In general, we deal here with a broader definition of *ratchet* transport, which can be obtained by breaking the reflection symmetry in space, or the reflection and shift symmetries in time. Notably this is possible by a proper choice of $E(t)$ alone. Thus, it turns out not to be necessary to break the reflection symmetry of the periodic potential $U(x)$. Of course one can also break all symmetries in time and space simultaneously, which may lead to a quantitative change of the results.

We consider the case of a simple potential $U(x) = -\cos(2\pi x)$ and a driving force which contains three harmonics:

$$E(t) = E_1 \cos(\omega t) + E_2 \cos(2\omega t + \phi_2) + E_3 \cos(3\omega t + \phi_3). \tag{4}$$

Here and in the following we choose $T = 2\pi$ and $\omega = 1$.

For $E_2 = E_3 = 0$ both symmetries, $\hat{S}_1$ and $\hat{S}_2$, are present and the total current equals zero. For $E_2 = 0$, symmetry $\hat{S}_1$ is present and we have again zero current. For $E_3 = 0$ and $E_2 \not\equiv 0$ all symmetries are broken, except for the specific values $\phi_2 = k\pi$, $k = 0, 1, 2, \ldots$, and, in general, we can expect a nonzero current in the system (1). In Fig. 1a, we show the time dependence of the coordinate $x(t)$ for several values of E_3 and nonzero values of E_1, E_2. The initial conditions are chosen to be within the main stochastic layer (see [16] and Figs. 2 and 3). An interesting effect results from the variation of E_3: the increase of E_3 from 0 to 0.3 leads to a current reversal, which is the result of a nonlinear interaction of harmonics. Thus, for some value of E_3 between $E_3 = 0$ and 0.3, the average

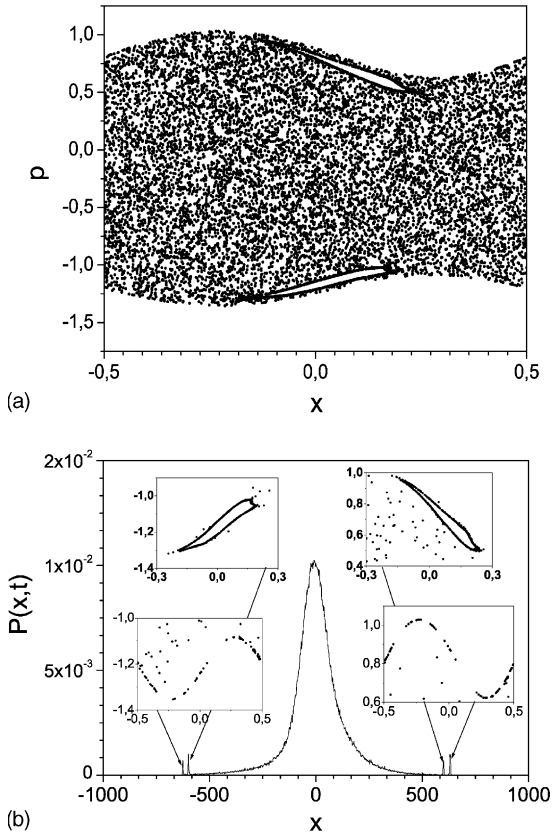

Fig. 2. (a) Poincaré section and (b) the propagator for a fixed time ($t = 100T$) for $E_3 = 0.143$ (case B).

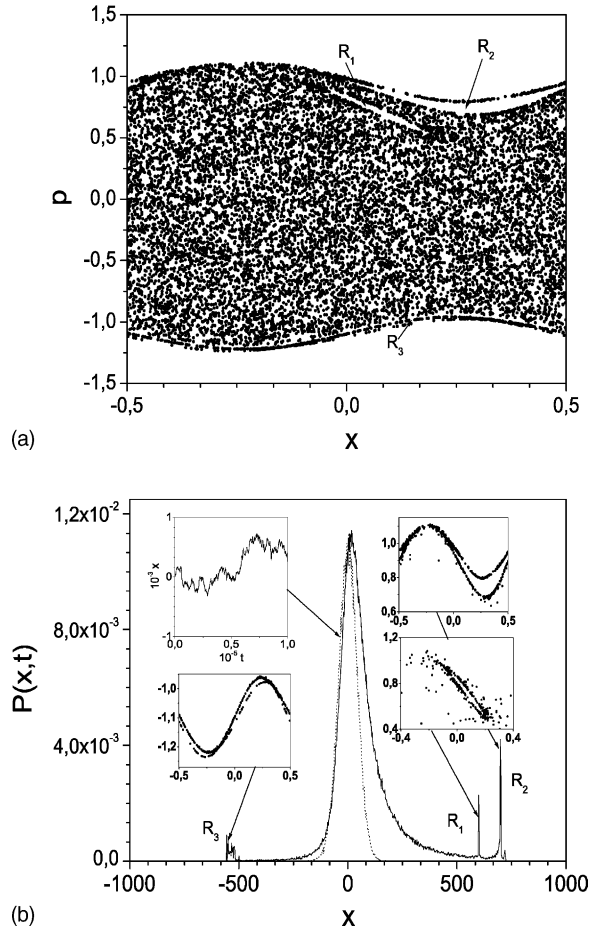

Fig. 3. Same as in Fig. 2 for $E_3 = 0.3$ (case C). Dashed line corresponds to the propagator for a dynamical process without flights in the ballistic channels R_1, R_2 and R_3 (see text). The right upper inset displays zooming of the corresponding trajectory.

velocity of any trajectory in the layer should be equal to zero. This is the case for $E_3 \approx 0.143$. Thus, while all symmetries (2) and (3) are broken, we find zero current as the result of a balance between all microscopic dynamical mechanisms.

The dynamics of trajectories in the stochastic layer appears to be complex. The insets in Fig. 1a show that in parts the particle evolves in seemingly free ballistic flights of different lengths. A Poincaré map of one such flight shows that the trajectory in the stochastic layer sticks to resonances. Since any reasonable statistics for a single trajectory can be obtained only after very long simulation times, a natural next step would be to consider the evolution of the distributions of many different trajectories. While the computational efforts will not be significantly lowered, such an analysis may in fact elucidate some peculiarities of the dynamics in a clear way. A first step would be to study an ensemble of trajectories which are described by a certain distribution function $\rho(p, x, t)$. We choose an initial distribution which is Maxwellian in p and homogeneous in x inside one spatial period of $U(x)$:

$$\rho(p, x, 0) = \frac{1}{L}\sqrt{\frac{\beta}{2\pi}}\, \mathrm{e}^{-(\beta/2)p^2}\Theta(x)\Theta(L - x) \tag{5}$$

with $\beta = 10$. This choice ensures that almost all trajectories are located inside the main stochastic layer. In Fig. 1b, we show the resulting reduced distributions $\rho_x(x,t) = \int_{-\infty}^{\infty} \rho(p,x,t=500T)\,\mathrm{d}p$, where 10^4 trajectories have been simulated. These distributions are characterized by a broad peak which is shifted to nonzero x values for the cases $E_3 = 0, 0.3$ and by some non-Gaussian tails. Such a representation could suggest that the above-mentioned ballistic flights are responsible for the tails, while the overall shift of the peak might be due to some purely diffusive processes. It should also be mentioned that ballistic flights may have different durations. Thus many trajectories experiencing ballistic flights also contribute to the central peak position. Consequently, we need more sophisticated statistical techniques to explore the peculiarities of the dynamics and to find the true sources for the observed transport properties. We conclude this section with stating that the computed average position $X(t) = \int x\rho_x(x,t)\,\mathrm{d}x$ yields a drift velocity $X(t)/t$ which is close to the one obtained from a single long trajectory.

3. The role of ballistic channels

The nonlinear Hamiltonian system (Eq. (1)) has a mixed phase space, which contains a main stochastic layer and regular resonance islands [21]. These islands are impermeable for chaotic trajectories and, at a first glance, can be excluded from the phase space, which would result in a complete separation of the ergodic component of motion from the non-ergodic one. In reality, such a separation is impossible because of the complex phase space structure of the boundaries between the chaotic and regular regions. Close to resonances the chaotic layer contains hierarchical sets of *cantori*, which form complex bottleneck-like barriers, through which orbits can penetrate. Due to the cantori structure, a trajectory can be trapped for a long time near the corresponding resonance. The sticking effect leads to the appearance of long regular flights which alternate with chaotic motion. For a nonzero winding number υ, these phases correspond to long unidirectional flights. The case of $\upsilon = 0$ corresponds to a localized rotating motion [21]. Thus a resonance with $\upsilon \not\equiv 0$ forms a set of ballistic channels in the chaotic layer, and sticking to such a resonance corresponds to a trapping of the particle in this channel. This would lead us later to Lévy flights [17–19].

A possible way of obtaining a nonzero current can be realized through modes of motion with long-time correlations, where the characteristic time of correlation decay is much larger than the period of external driving T. In the stochastic layer, such modes can be associated with ballistic flights only. On the basis of these arguments, we may state that the flights inside ballistic channels play a crucial role in the process of current generation inside the chaotic layer. The key mechanism of current rectification is thus related to the symmetry breaking of the non-chaotic fraction of dynamics. Another possibility is that the purely diffusive dynamics inside the stochastic layer also contributes to a directed current [14]. We will show that this possibility is excluded in the cases under consideration.

Breaking the symmetry of ballistic flights implies that there is an asymmetry of resonance structures and that the value of the current should provide a quantitative measure of this asymmetry. For the analysis of the system's dynamics, we used the propagator $P(x,t)$, i.e. the probability density for a particle to move over distance x during time t.[2] In Figs. 2b and 3b, we show the propagator for a fixed time $t = 100T$ which was obtained using a long chaotic trajectory with the duration $10^7 T$. This trajectory, due to ergodicity condition, covers the stochastic layer uniformly. The propagator structure has two prominent features: a central "bell-shaped" part and several sharp asymmetric peaks in the tails. These peaks correspond to flights which a particle performs when it sticks to a ballistic resonance. The peak location is exactly determined by the corresponding resonance winding number. It

[2] There is a difference between the propagator $P(x,t)$ and function $\rho(p,x,t)$ discussed in Section 2: $\rho(p,x,t)$ takes into account trajectories weighted over the *whole* phase space (including resonance islands and KAM-tori), whereas the propagator $P(x,t)$ includes only trajectories initiated at the chaotic layer.

is easy to identify all relevant ballistic channels using the propagator for a given time and stroboscopic Poincaré section (see Figs. 2a and 3a). For clarity, we emphasize that also the central part of the propagator at a given time contains contributions from flights. In other words, the propagator has a quite interesting dependence on the fixed time t. Nevertheless, it allows to observe the relevant ballistic channels which contribute for the chosen fixed time t.

For $E_3 = 0.3$, the resonance structure has a well-pronounced asymmetry, which becomes evident in the asymmetry of the propagator. There are two ballistic channels for positive direction: R_1 with winding number $\upsilon_2 = 6/T \approx 0.955$ and R_2 with $\upsilon_1 = 7/T \approx 1.115$ and only one for negative direction, R_3 with winding number $\upsilon_3 = -22/4T \approx -0.876$. As a result we observe a positive current.

Now we show that a nonzero current is indeed fully determined by the sticking to ballistic channels. We simply eliminate all ballistic flights from the dynamics of any trajectory by using a velocity gated technique. We take into account the existence of channels R_1, R_2 and R_3. After successive waiting times of $10T$, we test whether the spatial shift corresponds to a sticking in a given ballistic channel with a known winding number and an uncertainty of 5%. If we apply this filtering to a single trajectory, we observe practically zero current $J \approx -0.005$ (see dotted line in Fig. 1). The resulting reduced propagator is shown as a dashed line in Fig. 3. It is clearly symmetrical. Thus, we conclude that within an uncertainty of 5% purely diffusive motion does not contribute to the induced current. In fact we argue that even these possible 5% are due to smaller resonances and higher-order ballistic channels embedded in the stochastic layer.

In contrast to the previous case, the propagator for $E_3 = 0.143$ is symmetrical, which corresponds to zero current. This is the consequence of the fully symmetrical resonance structure for which the resonances with opposite winding number compensate each other. Thus, in this case the zero current value is the result of a *dynamical* symmetry rather than a *geometrical* asymmetry $E(t)$ defined in Eqs. (2) and (3).

4. Generalized asymmetric CTRW model

In order to quantify our result that the observed current results from ballistic flights (corresponding to long correlations), while random diffusion (corresponding to fast decay of correlations) gives no contribution to the total current, we simulate the dynamics by a sequence of alternating processes: *flights* (sticking to ballistic channels) and unbiased *random walk* (chaotic diffusion in random area). It is reasonable to assume that there is no correlation between flights because successive flights are usually separated by a diffusive component. Using these assumptions, the dynamics can be effectively modeled within the CTRW formalism [22] as a generalized asymmetrical flight process [23].

Let as assume that there are N relevant different resonances with winding numbers υ_i, $i = 1, \ldots, N$. Every resonance is characterized by a PDF with sticking time $\psi_i(t)$ and probability of sticking event p_i. The random walk phase is characterized by a PDF $\psi_c(t)$. Using a standard scheme (see Appendix A for details), we obtain the following expression for the current:

$$J = \frac{\sum_{i=1}^{N} p_i \upsilon_i \langle t_i \rangle}{\sum_{i}^{N} p_i \langle t_i \rangle + \langle t_c \rangle}, \tag{6}$$

where $\langle t_i \rangle = \int_0^\infty t \psi_i(t)\, \mathrm{d}t$ and $\langle t_c \rangle = \int_0^\infty t \psi_c(t)\, \mathrm{d}t$. All the first moments are finite due to the Kac theorem on the finiteness of recurrence times in Hamiltonian systems [21].

The contribution of a single flight in the ith channel is given by

$$\Psi_i(x, t) = \delta(x - \upsilon_i t)\psi_i(t). \tag{7}$$

The propagator for the random diffusion reads as

$$\Psi_{\mathrm{c}}(x,t) = \frac{1}{\sqrt{\pi D t}}\,\mathrm{e}^{-x^2/Dt}\psi_{\mathrm{c}}(t). \tag{8}$$

The total propagator for the time $t = MT$ is a convolution of single motion events (7) and (8):

$$P(x,MT) = Q\sum_{n=1}^{M}\sum_{k=1}^{M-n}\cdots\sum_{l=1}^{M-n-\cdots-g}\Psi_{\mathrm{c}}(x,(M-n-\cdots-l)T)\Psi_1(x,nT)\cdots\Psi_N(x,lT), \tag{9}$$

where the number of sums equals to the number of ballistic channels N and Q is normalization constant.

Let us consider in details the case when $E_3 = 0.3$ for which there are three relevant ballistic channels, R_1, R_2 and R_3. Since winding numbers of all resonances are known, we can separate those parts of the trajectories, which correspond to particle flights in a certain channel. This has been done numerically by identifying an elementary flight using a velocity gate. We use here the same procedure as used above for filtering. The corresponding sticking time PDF for resonances R_1 and R_2 are shown in Fig. 4. Sticking to the resonance R_3 is extremely rare, and the characteristic time spent by the particle in this channel is much smaller than the characteristic time for channel R_2. Thus the influence of R_3 is negligible. Without any notable loss of precision, we can suggest that transport in negative direction is determined only by random diffusion.

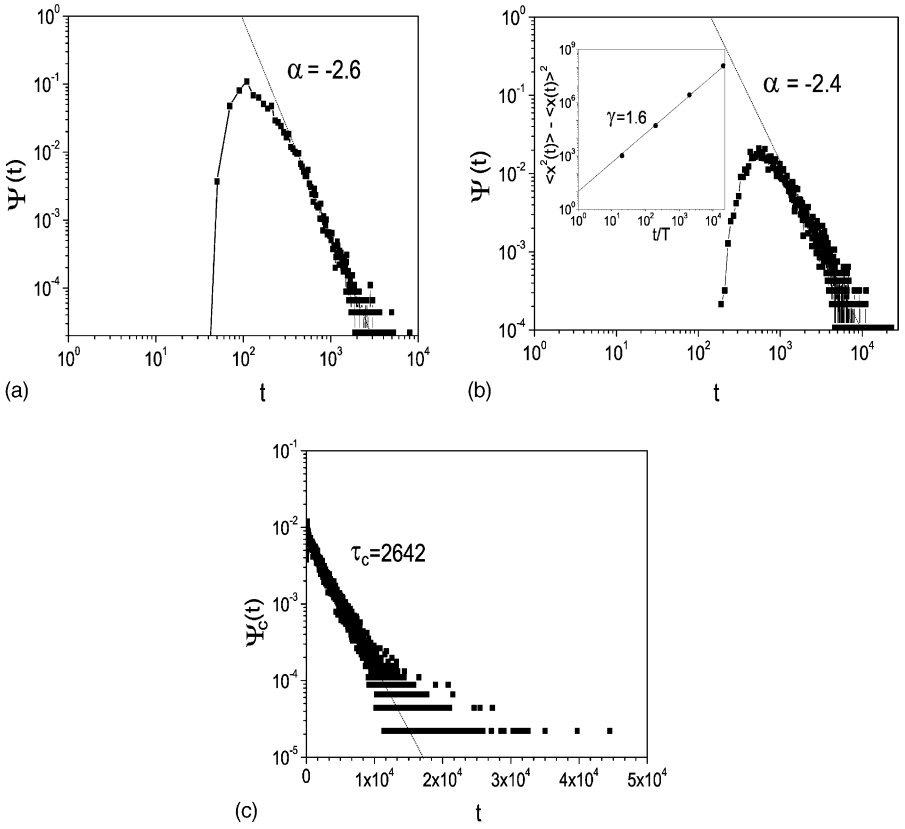

Fig. 4. The numerically obtained sticking time PDF for: (a) R_1, (b) R_2, and (c) random walk phase for $E_3 = 0.3$ (see text). Inset in (c) shows the mean square evolution for the global diffusion into the chaotic layer.

Both PDFs for R_1 and R_2 have power-like tails: $\psi_{1,2} \sim t^{-\alpha_{1,2}}$, $\alpha_1 \approx -2.6$, $\alpha_2 \approx -2.4$. Thus, we are confronted with the appearance of Lévy flights. Resonance R_1 has the most dominant contribution (the probability of sticking $p_1 = 0.94$) and its mean sticking time $\langle t_1 \rangle \approx 286$. Resonance R_2 has a sticking probability $p_2 = 0.06$ and a mean sticking time $\langle t_2 \rangle \approx 1673$. Thus, though the particle gets relatively seldom into the ballistic channel R_2, it spends there a time which is almost one order of magnitude larger then the characteristic sticking time for channel R_1. The resonance R_2 shows up with a stronger anomalous character than R_1 and therefore this resonance determines the asymptotic of the global diffusion in the stochastic layer. The evolution of the corresponding variance of the mean square displacement $\langle x^2 \rangle - \langle x \rangle^2 \sim t^\gamma$ is shown as an inset in Fig. 4b. The diffusion has strong anomalous character with a characteristic exponent $\gamma \approx 1.6$, which is in agreement with the exponent α_2 ($\gamma = 4 - \alpha_2$) [22]. Numerical analysis of the random walk PDF $\psi_c(t)$ demonstrates a well-pronounced Poissonian distribution:

$$\psi_c(t) = \frac{1}{\tau_c} \mathrm{e}^{-t/\tau_c} \tag{10}$$

with a time constant $\tau_c \approx 2642$, which is equal to the mean time of a random diffusion process. Using the numerical values of the relevant parameters, Eq. (6) for the current gives $J_{\mathrm{num}} \approx 0.118$, which is very close to the result of direct numerical integration of (1) (see Fig. 1a).

Using the exponents α_1 and α_2, we simulate the dynamics within the chaotic layer by a CTRW process with the following PDF distribution:[3]

$$\psi_{1,2} = \begin{cases} 0, & t < t_c^{1,2}, \\ A_{1,2} t^{-\alpha_{1,2}}, & t \geq t_c^{1,2}, \end{cases} \tag{11}$$

where $t_c^1 = 115$, $t_c^2 = 530$, and the mean time $\langle t \rangle = t_c(\alpha - 1)/(\alpha - 2)$. In order to model the diffusional part, we used a Langevin equation with the diffusion coefficient $D = 1.6$ and the Poisson distribution (10) for the duration time of chaotic walking. The obtained trajectory is very close to the real trajectory (dotted line in Fig. 1a).

5. Conclusion

We have studied the mechanism of current rectification in AC-driven Hamiltonian systems. We found that directed transport inside the main chaotic layer is determined by breaking the symmetry of Lévy flights inside ballistic channels, which are generated due to the presence of resonance islands with nonzero winding numbers. This suggests a rather simple algorithm for estimating and controlling the current in the system. Namely, using the Poincaré section and the propagator $P(x, t)$, one can identify the relevant resonance islands and calculate their winding numbers. Then, by changing system parameters one can vary the resonance structure by opening and closing relevant ballistic channels.

We have found also that the nonlinear interaction between different harmonics of the driving force $E(t)$ can trigger a nontrivial current inversion in Hamiltonian systems. This change of sign is related to the appearance and disappearance of resonant islands.

In spite of the simple form of the Hamiltonian (1), we believe that the proposed mechanism is general. For example, the flight mechanism of current rectification can be probably realized in two-dimensional chaotic advection systems [24]. The phase space of this Hamiltonian system is mixed and shows up with a variety of Lévy flights in its dynamics [25].

[3] For generation of random variable x with distribution (11) we have used the random variable ξ with uniform distribution in unit interval and transformation $x = t_c \xi^{-1/(\alpha-1)}$.

The resonance sticking mechanism can be important for the semi-classical quantum version of Hamiltonian systems. In this case sticking can be also realized, which is due to the presence of a new class of hierarchical eigenstates [26,27]. The resonance structure asymmetry can lead to the appearance of a nonzero current in this case. These effects can be implemented experimentally, e.g. in a system of cold cesium atoms [8,28]. The dynamics of an atomic ensemble under the influence of a laser radiation can be described rather well by a classical Hamiltonian, and the quantum–classical correspondence time is about $50T$ [8], which is sufficient for the observation of the effects discussed above.

The system coordinate $x(t)$ can represent not only a translational degree of freedom but also a rotational one. In that case, a Hamiltonian similar to (1) is capable of describing the dynamics of single molecules under the influence of electromagnetic radiation. If the corresponding molecular gas density is low enough, a cloud of spinning molecules can serve as a high-frequency modulator with controlled chirality.

Acknowledgements

One of the author (SF) thanks M. Fistul (MPIPKS) for helpful discussions and a careful reading of the manuscript. Financial support from the Israel Science Foundation, the USA Israeli Binational Foundation, and DIP and SISIT-OMAS grants is gratefully acknowledged.

Appendix A

Let $P(x,t)$ be a propagator for a random walker position for large times. The first moment of x is obtained from the Fourier transform of $P(x,t)$:

$$\mathrm{i}\frac{\partial P(k,t)}{\partial k}\bigg|_{k=0} = \langle x(t)\rangle. \tag{A.1}$$

We now introduce some relevant definitions.

The probability density that a flight event has a distance of x and duration t:

$$\xi(x,t) = \sum_{i=1}^{N} p_i \delta(x - v_i t)\psi_i(t).$$

The probability that the particle has moved a distance x in time t in a single flight (not necessarily stopping):

$$\Gamma(x,t) = \sum_{i=1}^{N} p_i \delta(x - v_i t)\int_t^\infty \psi_i(\tau)\,\mathrm{d}\tau.$$

The probability that the particle performs a random walk for at least time t (and remains walking):

$$\Phi(t) = \int_\infty^t \psi_c(\tau)\,\mathrm{d}\tau.$$

The probability of just starting a random walk at (x,t):

$$Y(x,t) = \frac{1}{2}\delta(t)\delta(x) + \int_{-\infty}^{\infty}\mathrm{d}x'\int_0^t \mathrm{d}t'\,Z(x',t')\xi(x-x',t-t'),$$

where $Z(x,t)$ describes the probability of just starting a flight at (x,t):

$$Z(x,t) = \frac{1}{2}\delta(t)\delta(x) + \int_0^t \mathrm{d}t'\, Y(x',t')\psi_{\mathrm{c}}(t-t').$$

The final equation for $P(x,t)$ is therefore

$$P(x,t) = \int_0^t \mathrm{d}t'\, \Phi(t-t')Y(x,t') + \int_0^\infty \mathrm{d}x' \int_0^t \Gamma(x-x',t-t')Z(x',t'). \tag{A.2}$$

The integral equation (A.2) can be solved by Fourier transforming space and Laplace transforming time. Thus

$$P(k,s) = \{s^{-1}[1-\psi_s(s)]\}\left[\frac{\frac{1}{2}+\frac{1}{2}\xi(k,s)}{1-\xi(k,s)\psi_s(s)}\right] + \left[\sum_{i=1}^N p_i\lambda_i\right]\left[\frac{\frac{1}{2}+\frac{1}{2}\psi_s(s)}{1-\xi(k,s)\psi_s(s)}\right],$$

where $\xi(k,s) = \sum_{i=1}^N p_i\psi_i(s+\mathrm{j}kv_i)$, $\lambda_i(k,s) = p_i(s+\mathrm{j}kv_i)^{-1}[1-\psi_i(s+\mathrm{j}kv_i)]$, and j is the imaginary unit.

Thus

$$\langle x\rangle = \frac{(1+\psi_{\mathrm{c}})\sum_{i=1}^N p_i v_i(1-\psi_i(s))}{2s^2(1-\xi\psi_{\mathrm{c}})}. \tag{A.3}$$

All functions $\psi_i(t)$ and $\psi_{\mathrm{c}}(t)$ must have a finite first moment (because of the Kac theorem about finiteness of recurrence times in Hamiltonian systems [21]). Thus, for small s (that corresponds to $t\to\infty$)

$$\psi_i(s) = 1 - s\langle t_i\rangle + \cdots, \qquad \psi_{\mathrm{c}}(s) = 1 - s\langle t_s\rangle + \cdots. \tag{A.4}$$

Using expansion (A.4) we obtain from (A.3):

$$\langle x(s)\rangle = \frac{\sum_{i=1}^N p_i v_i\langle t_i\rangle}{\sum_i^N p_i\langle t_i\rangle + \langle t_{\mathrm{c}}\rangle}\frac{2-s\langle t_{\mathrm{c}}\rangle}{2s^2} \approx \frac{\sum_{i=1}^N p_i v_i\langle t_i\rangle}{\sum_i^N p_i\langle t_i\rangle + \langle t_{\mathrm{c}}\rangle}\frac{1}{s^2}.$$

This leads to

$$\langle x(t)\rangle = \frac{\sum_{i=1}^N p_i v_i\langle t_i\rangle}{\sum_i^N p_i\langle t_i\rangle + \langle t_{\mathrm{c}}\rangle}t,$$

and, finally, we obtain for the asymptotic current

$$J = \frac{\sum_{i=1}^N p_i v_i\langle t_i\rangle}{\sum_i^N p_i\langle t_i\rangle + \langle t_{\mathrm{c}}\rangle}. \tag{A.5}$$

References

[1] R.Z. Sagdeev, D.A. Usikov, G.M. Zaslavsky, Nonlinear Physics: from the Pendulum to Turbulence and Chaos, Harwood, New York, 1992; S. Wiggins, Chaotic Transport in Dynamical Systems, Springer, Berlin, 1992.
[2] P. Hänggi, R. Bartussek, in: J. Parisi, S.C. Muller, W. Zimmermann (Eds.), Nonlinear Physics of Complex Systems, Lecture Notes in Physics, Vol. 476, Springer, Berlin, 1996, p. 294.
[3] S. Flach, O. Yevtushenko, Y. Zolotaryuk, Phys. Rev. Lett. 84 (2000) 2358.
[4] J.L. Mateos, Phys. Rev. Lett. 84 (2000) 258.
[5] M. Porto, M. Urbakh, J. Klafter, Phys. Rev. Lett. 85 (2000) 491.
[6] M. Barbi, M. Salerno, Phys. Rev. E 62 (2000) 1988.
[7] P. Reimann, Phys. Rep. 361 (2002) 57.
[8] I. Zapata, R. Bartussek, F. Sols, P. Hänggi, Phys. Rev. Lett. 77 (1996) 2292.

[9] F.L. Moore, et al., Phys. Rev. Lett. 75 (1995) 4598;
J.C. Robinson, et al., Phys. Rev. Lett. 76 (1996) 3304.
[10] Y.M. Blanter, M. Büttiker, Phys. Rev. Lett. 82 (1999) 851.
[11] S. Grossmann, H. Fujisaka, Phys. Rev. A 26 (1982) 1179;
P. Gaspard, J. Statist. Phys. 68 (1992) 673.
[12] P. Jung, J.G. Kissner, P. Hänggi, Phys. Rev. Lett. 76 (1996) 3436;
Ya.M. Blanter, M. Bütiker, Phys. Rev. Lett. 81 (1998) 4040.
[13] I. Goychuk, P. Hänggi, in: J. Freund, T. Poeschel (Eds.), Stochastic Processes in Physics, Lectures Notes in Physics, Vol. 557, Springer, Berlin, 2000, p. 7;
T. Dittrich, R. Ketzmerick, M.-F. Otto, H. Schanz, Ann. Phys. (Leipzig) 9 (2000) 755.
[14] H. Schanz, M.-F. Otto, R. Ketzmerick, T. Dittrich, Phys. Rev. Lett. 87 (2001) 07601.
[15] O. Yevtushenko, S. Flach, A.A. Ovchinnikov, Y. Zolotaryuk, Europhys. Lett. 54 (2) (2001) 141.
[16] S. Denisov, S. Flach, Phys. Rev. E 64 (2001) 056236.
[17] M.F. Shlesinger, G.M. Zaslavsky, J. Klafter, Nature 363 (1993) 31.
[18] J. Klafter, M.F. Shlesinger, G. Zumofen, Phys. Today 49 (1996) 33.
[19] T. Geisel, A. Zacherl, G. Radons, Phys. Rev. Lett. 59 (1987) 2503.
[20] M. Glück, A.R. Kolovsky, H.J. Korsch, Physica D 116 (1998) 283.
[21] G.M. Zaslavsky, Physics of Chaos in Hamiltonian Systems, Imperial College Press, 1998.
[22] G. Zumofen, J. Klafter, A. Blumen, Phys. Rev. E 47 (1993) 2183;
J. Klafter, G. Zumofen, Phys. Rev. E 49 (1994) 4873.
[23] E.R. Weeks, H.L. Swinney, Phys. Rev. E 57 (1998) 4915.
[24] W. Young, A. Pumir, Y. Pomeau, Phys. Fluids A 1 (1989) 462;
J.M. Ottino, Phys. Fluids 31 (1988) 1372.
[25] T.H. Solomon, E.R. Weeks, H.L. Swinney, Phys. Rev. Lett. 71 (1993) 3978;
T.H. Solomon, E.R. Weeks, H.L. Swinney, Physica D 76 (1994) 70.
[26] R. Ketzmerick, L. Hufnagel, F. Steinbach, M. Weiss, Phys. Rev. Lett. 85 (2000) 1214.
[27] A. Iomin, G.M. Zaslavsky, Chaos 10 (2000) 147.
[28] B.G. Klappauf, W.H. Oskay, D.A. Steck, M.G. Raizen, Phys. Rev. Lett. 81 (1998) 4044.